

Active debris removal space mission concepts based on hybrid propulsion

Original

Active debris removal space mission concepts based on hybrid propulsion / Tadini, P.; Tancredi, U.; Grassi, M.; Anselmo, L.; Pardini, C.; Branz, F.; Francesconi, A.; Maggi, F.; Lavagna, M.; De Luca, L. T.; Viola, Nicole; Chiesa, Sergio; Trushlyakov, V.; Shimada, T.. - ELETTRONICO. - 3:(2013), pp. 2319-2328. (Intervento presentato al convegno 64th International Astronautical Congress 2013, IAC 2013 tenutosi a Beijing, chn nel 2013).

Availability:

This version is available at: 11583/2656245 since: 2016-11-17T12:23:38Z

Publisher:

International Astronautical Federation, IAF

Published

DOI:

Terms of use:

This article is made available under terms and conditions as specified in the corresponding bibliographic description in the repository

Publisher copyright

(Article begins on next page)

IAC-13-A6.6.5

ACTIVE DEBRIS REMOVAL SPACE MISSION CONCEPTS BASED ON HYBRID PROPULSION

P. Tadini¹, U. Tancredi², M. Grassi³, L. Anselmo⁴, C. Pardini⁴, F. Branz⁵, A. Francesconi⁵, F. Maggi¹, M. Lavagna¹, L.T. De Luca¹, N. Viola⁶, S. Chiesa⁶, V. Trushlyakov⁷ and T. Shimada⁸

¹Politecnico di Milano, Milan, Italy, pietro.tadini@polimi.it, filippo.maggi@polimi.it,
michelle.lavagna@polimi.it, luigi.deluca@polimi.it

²University of Naples "Parthenope", Naples, Italy, urbano.tancredi@uniparthenope.it

³University of Naples "Federico II", Naples, Italy, michele.grassi@unina.it

⁴ISTI - Consiglio Nazionale delle Ricerche (CNR), Pisa, Italy, luciano.anselmo@isti.cnr.it,
carmen.pardini@isti.cnr.it

⁵University of Padua, Padua, Italy, francesco.branz@unipd.it, alessandro.francesconi@unipd.it

⁶Politecnico di Torino, Turin, Italy, nicole.viola@polito.it, sergio.chiesa@polito.it

⁷Omsk State Technical University, Omsk, Russia, trushlyakov@omgtu.ru

⁸Institute of Space and Astronautical Science (JAXA), Sagami-hara, Japan, shimada.toru@jaxa.jp

During the last 40 years, the mass of the artificial objects in orbit increased quite steadily at the rate of about 145 metric tons annually, leading to about 7000 metric tons. Most of the cross-sectional area and mass (97% in low Earth orbit) is concentrated in about 4500 intact abandoned objects plus a further 1000 operational spacecraft. Analyses have shown that the most effective mitigation strategy should focus on the disposal of objects with larger cross-sectional area and mass from densely populated orbits. Recent NASA results have shown that the worldwide adoption of mitigation measures in conjunction with active yearly removal of approximately 0.2–0.5% of the abandoned objects would stabilize the debris population. Targets would have typical masses between 500 and 1000 kg in the case of spacecraft, and of more than 1000 kg for rocket upper stages. In the case of Cosmos-3M second stages, more than one object is located nearly in the same orbital plane. This provides the opportunity of multi-removal missions, more suitable for yearly removal rate and cost reduction needs.

This paper deals with the feasibility study of a mission for the active removal of large abandoned objects in low Earth orbit. In particular, a mission is studied in which the removal of two Cosmos-3M second stages, that are numerous in low Earth orbit, is considered. The removal system relies on a Chaser spacecraft which performs rendezvous maneuvers with the two targets. The first Cosmos-3M stage is captured and an autonomous de-orbiting kit, carried by the Chaser, is attached to it. The de-orbiting kit consists of a Hybrid Propulsion Module, which is ignited to perform stage disposal and controlled reentry after Chaser separation. Then, the second Cosmos-3M stage is captured and, in this case, the primary propulsion system of the Chaser is used for the disposal of the mated configuration. Critical mission aspects and related technologies are investigated at a preliminary level. In particular, an innovative electro-adhesive system for target capture, mechanical systems for the hard docking with the target and a hybrid propulsion technology suitable for rendezvous, de-orbiting and controlled reentry operations are analyzed. This is performed on the basis of a preliminary mission profile, in which suitable rendezvous and disposal strategies have been considered and investigated by numerical analysis. A preliminary system mass budget is also performed, showing that the Chaser overall mass is about 1350 kg, including a primary propulsion system of about 300 kg, and a de-orbiting kit with a mass of about 200 kg. The system designed results suitable to be launched with VEGA, actually the cheapest European space launcher.

I. INTRODUCTION

As of 14 May 2013, 3738 payloads and 1965 rocket bodies orbited the Earth¹. Taking into account that approximately 1050 spacecraft were operational, there were around 4650 intact payloads and rocket bodies abandoned in the circumterrestrial space. In Low Earth Orbit (LEO), i.e. below the altitude of 2000 km, where the orbital object and debris density is maximum, there were 1939 payloads and 813 rocket bodies, of which about 2250 completely abandoned. Therefore, more than 48% of the intact spacecraft and upper stages resided entirely in LEO, and this also applied to the abandoned objects.

The extrapolated total mass in orbit^{2,3} was around 6670 metric tons, including the International Space Station (420 metric tons). It was mainly concentrated in spacecraft (53.3%) and upper stages (42.5%), while mission related objects accounted for only 2.5% and orbital fragments for 1.7%¹. Excluding the International Space Station (ISS), the total mass in LEO was approximately 2650 metric tons, of which about 97% concentrated in payloads and rocket bodies¹. Overall, the average payload mass was 950 kg, ISS included, and 838 kg, ISS excluded, while rocket bodies had an average mass of 1442 kg¹. Ignoring the ISS, the average mass of intact spacecraft and upper stages currently in

space is 1046 kg, reduced to 934 kg for the objects entirely resident in LEO, i.e. with a mean altitude lower than 2000 km¹.

During the last decade, several detailed parametric simulations have shown that the most effective way to prevent the further long-term growth of debris larger than 10 cm, able to cause the catastrophic collisional breakup of an “average” 934 kg object in LEO, would be to remove mass from densely populated orbital regimes, in addition to the strict adoption of recommended mitigation guidelines⁴. In practice, the active yearly removal of approximately 0.2–0.5% of the abandoned intact objects in LEO would be sufficient, provided that the highest priority were given to the targets characterized by the highest products of catastrophic collision probability with debris (P_c) and target mass (M), i.e. $P_c \times M$ ^{3,5}.

In this regard, hybrid rocket technology might represent a valuable option^{1,6}. Once demonstrated the feasibility of hybrid propulsion and capture systems in space, the most important step would be the development of a multiple removal mission. According to current estimates, the removal of 5-10 objects per year would be probably sufficient to prevent the outbreak of the “Kessler Syndrome” in the next 200 years, consisting in the exponential growth of space debris. Hence the removal of two or more large abandoned objects with a single mission is a very important aspect, especially concerning the costs. The greatest cost of a space mission is related to the launcher and the propellant used to reach the selected orbit(s). The possibility of many removals with one single launch is the only way to promote the development of remediation missions.

In the Multi-Removal Mission a Chaser spacecraft, equipped with a Hybrid Rocket Engine (HRE) as primary propulsion, aims to achieve the contact with multiple targets, attaching on each one a Hybrid Propulsion Module (HPM), which performs the debris de-orbiting and controlled reentry. The HPM is the main component of the de-orbiting kit, which is composed even by a hard docking system, for the rigid connection with the target object, a monopropellant secondary propulsion system, for the attitude control, and the required avionics for the disposal.

II. TARGET SELECTION

The current distribution of abandoned intact spacecraft and upper stages in LEO is summarized in Figures 1 and 2. Together with the object ranking defined in the previous section, it suggests that optimal active debris removal missions should be preferentially carried out in a few critical altitude-inclination bands^{6,7}, characterized by heights in between 500 and 1100 km and inclinations $i > 64^\circ$.

A very attractive target for active removal is represented by the Russian Cosmos-3M second stages, with mass of 1400 kg, diameter of 2.4 m and length of 6.5 m, of which about 300 are in orbit, mainly concentrated in four critical altitude-inclination bands: 850-1050 km, $i = 83^\circ$; 900-1050 km, $i = 66^\circ$; 900-1000 km, $i = 74^\circ$; and 650-850 km, $i = 74^\circ$ (Figures 1 and 2).

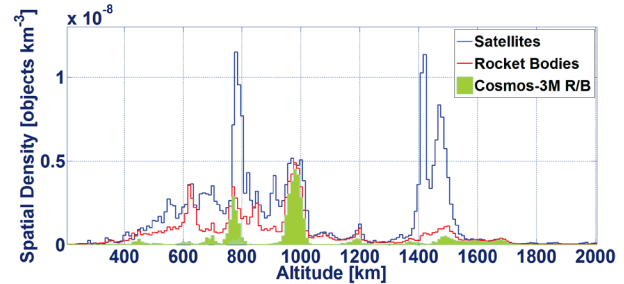


Fig. 1: Spatial density in LEO of intact satellites and rocket bodies. The distribution of Cosmos-3M second stages is highlighted as well.

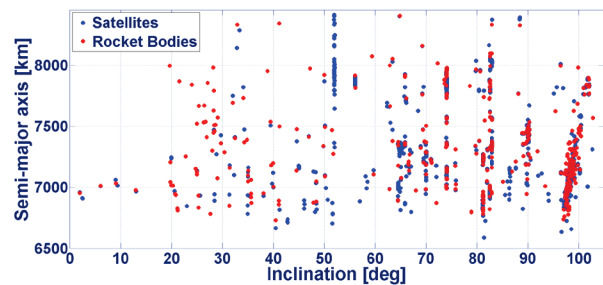


Fig. 2: Distribution of intact satellites and rocket bodies fully residing in LEO as a function of semi-major axis and inclination. The Earth’s equatorial radius is about 6378 km.

The targeting of this upper stage presents quite evident advantages: among them, the same capture techniques and procedures might be used many times over decades, it would be possible to operate in at least four separate altitude-inclination critical bands, the reentry risk assessment for de-orbiting (fragmentation analysis) should be carried out for only one object representative of the entire class, and the reduced set of de-orbiting kits needed might be tailored for small series production. In addition, multiple rendezvous might be possible within a single mission, because, for any given inclination, an average of about two stages would be present in each 5° bin of right ascension of the ascending node (Ω), with more favorable concentrations around specific orbit planes (Figure 3). Last, but not least, the choice of the Cosmos-3M second stages as targets for active debris removal would offer the occasion for a broad cooperation with Russia, concerning both the rocket body itself (Omsk State

Technical University) and the eventual availability of launchers at low cost (Dnepr, Rokot) for the removal missions.

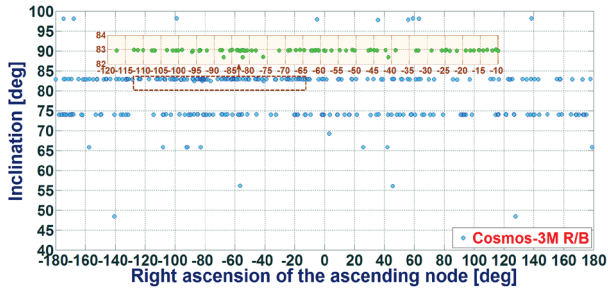


Fig. 3: Dispersion of the orbital planes of the Cosmos-3M rocket bodies (R/B) in LEO (19 July 2012).

In order to select suitable targets for a demonstrative two-removal mission, all the Cosmos-3M second stages present in the inclination bands of 74° and 83° have been considered. Since one of the main design requirements of a multi-removal mission is to limit the Chaser out-of-plane maneuvers needed for the rendezvous with multiple targets, these objects have been filtered considering a $\Delta\Omega$ difference of less than 1°. Around the inclination of 74° the average altitude of the objects is between 750 and 780 km, whereas around 83° the average altitude is between 950 and 990 km. In the latter inclination band many couples of stages with a small $\Delta\Omega$ are present, while just 8 couples were identified in the former band. The stage couple selected for developing the multi-removal mission concept consists of Cosmos-3M 11112 and Cosmos-3M 22676, respectively at an average altitude of 767.62 km and 777.97 km in the first inclination band.

III. MISSION CONCEPT

A multi-removal mission involves several steps and critical aspects. First of all, an effective rendezvous (RV) strategy is required, especially in the close-range when the Chaser is at a distance of a few meters from the target. The close-range RV maneuver is indeed very important for target capture by means of the soft docking system described in the next section. In addition, in order to perform debris disposal, the de-orbiting kit carried by the Chaser must be safely connected to the target external structure.

In order to perform preliminary analyses, a demonstrative two-removal mission has been considered, whose profile can be summarized by the following main steps:

1. The Chaser is released by the launcher on a LEO parking orbit;

2. The Chaser performs the RV with the first target using the HRE;
3. The first target is captured and a de-orbiting kit is rigidly connected to its nozzle. These operations are performed by a soft docking system and a robotic arm, which aligns the HPM (de-orbiting kit) with the nozzle of the target;
4. The Chaser leaves the first target and moves towards the second target;
5. The HPM on the first target is remotely ignited to perform the disposal;
6. The Chaser performs the RV with the second target;
7. The second target is captured with the soft docking system and the Chaser rigidly connects itself with the target nozzle;
8. The remaining propellant is used by the HRE to perform the disposal of the system target-Chaser.

Of course, in case of n removals, the steps from 2 to 6 shall be repeated $n-1$ times.

III.1 Rendezvous ΔV Budget

For RV preliminary analysis it is assumed that the Chaser is injected in a 700 km circular orbit in the same plane of the first target, i.e. the one at lower altitude (namely Cosmos-3M 11112). The considered RV maneuver profile consists of the following main phases:

1. The Chaser is maneuvered up to the first target with a two-burn Hohmann transfer, which brings the Chaser sufficiently near to the debris to start near-range RV;
2. The Chaser is maneuvered for mating with the stage, so to allow de-orbiting kit installation. This maneuver is not modeled, but it is assumed that it lasts about 48 hours;
3. The Chaser is detached from the first stage and maneuvered up to the second target. This is done by a three-impulse in-plane Hohmann maneuver (see schematic in Figure 4), for simultaneous phasing and orbit transfer, plus a plane change to null Δi and $\Delta\Omega$.

The analysis was carried out with the following assumptions:

- All orbits are circular (the small ~ 0.001 eccentricity was neglected);
- The target orbital elements refer to the time at which the first RV maneuver ends;
- The plane change maneuver is performed at the end of the three-impulse maneuver.

In order to reduce the overall RV ΔV budget, the Chaser phasing with the second target lasts 10 orbits, i.e. the Chaser performs 9 additional revolutions on the

second transfer orbit while phasing with the target. This yields the following equation relating the semi-major axes of the two transfer orbits, a_1 and a_2 , to the radius, r_{2D} , of the second target orbit, being N the number of revolutions for phasing ($N = 10$ in this case):

$$a_1^{3/2} + (2N - 1)a_2^{3/2} = 2 \left(N + \frac{\Delta v}{2\pi} \right) r_{2D}^{3/2} \quad [1]$$

By expressing a_2 as a function of a_1 and assuming that the starting and ending orbits are close (i.e. $r_{2D} - r_C \ll r_{2D}$), Eq.(1) becomes:

$$a_1^3 + \frac{3}{4} \left(2 - \frac{1}{N} \right) (r_{2D} - r_C) a_1^2 + \frac{9}{64} \left(2 - \frac{1}{N} \right)^2 \cdot (r_{2D} - r_C)^2 a_1 = \left(1 + \frac{\Delta v}{2N\pi} \right)^2 r_{2D}^3 \quad [2]$$

where r_C is the radius of the Chaser orbit at the end of the first RV maneuver. From Eq.(2) a_1 can be computed. According to the considered RV profile, the two RV maneuvers require about 36 m/s and 60 m/s, respectively. The total ΔV needed for RV is thus 96 m/s.

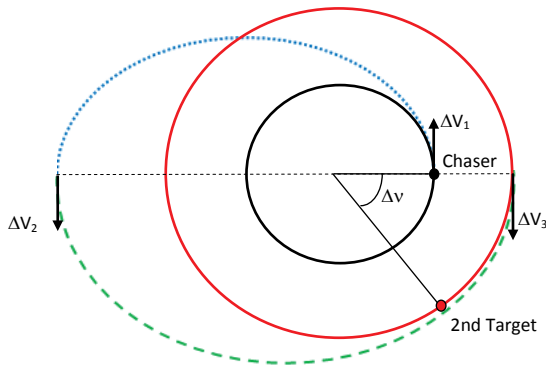


Fig. 4: Schematic of the three-impulse Hohmann RV maneuver.

III. II Disposal Analysis

Once the HPM is attached to the first debris, it is ignited to start the de-orbiting and reentry phase. Due to the large size and mass of the reentering objects, the destruction process in the atmosphere could be incomplete, with a high residual risk of ground impact. Hence, the reentry shall be controlled and directed to a specific location on Earth (usually uninhabited ocean regions). With reference to previous studies on LEO de-orbiting strategies¹, a disposal strategy is pursued in which the debris-HPM mated system is steered to an elliptical transfer orbit with a perigee sufficiently low so to allow an immediate atmospheric capture. In addition, to limit the ground impact area of fragments surviving the atmospheric entry, a sufficiently steep Flight Path Angle (FPA) is used.

For the disposal, both single burn and multi-burn

strategies could be used¹, even though the large size of the reentering objects suggests limiting the number of burns to allow an immediate reentry, so to relax the attitude control requirements of the mated configuration. Such a strategy is even more advisable for the disposal of the Chaser-debris mated configuration. Indeed, below 300 km the atmospheric torque can significantly affect the controlled reentry maneuver. In this paper, a preliminary, non-optimized, reentry trajectory analysis has been performed by assuming an elliptical reentry orbit with a perigee below 60 km and FPA $< -1.5^\circ$ at 120 km. The required ΔV magnitude, computed by assuming a Hohmann-transfer, is about 250 m/s (25% margin included). This value is used for HPM and HRE sizing, as well as for overall Chaser budgeting.

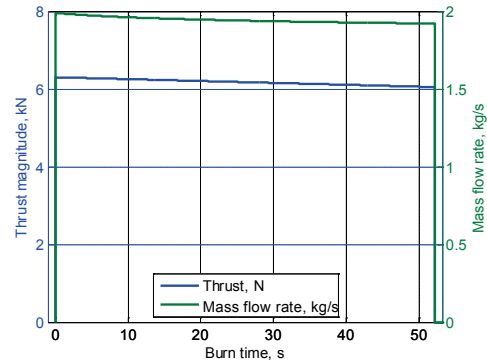


Fig. 5: Thrust profile for the DEO-Kit disposal.

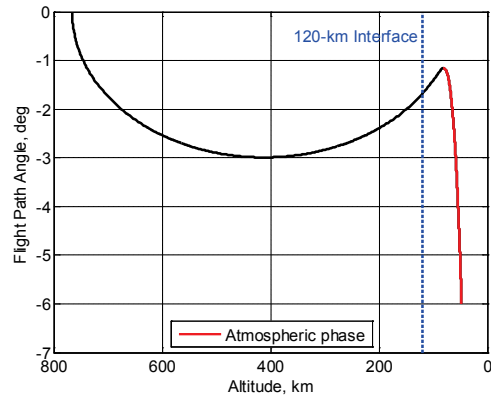


Fig. 6: FPA versus altitude.

Figures 5-7 show the results of the disposal analysis for the debris-HPM configuration (denoted as DEO-Kit in the following). More specifically, Figure 5 shows the adopted thrust profile, which allows keeping the average acceleration level within 0.4 g, thus reducing the debris fragmentation risk. Figures 6 and 7 show the FPA versus altitude and a summary of the overall de-orbiting maneuver. The FPA at 120 km is about -1.7° and the perigee altitude is about 59 km. Similar results are

achieved for the Chaser-debris mated configuration disposal, which are not shown for the sake of conciseness. It is worth mentioning that in this last case the average thrust is about 8 kN, determining an average acceleration level of about 0.35 g, the FPA at 120 km is about -1.8° and the perigee altitude is about 52 km.

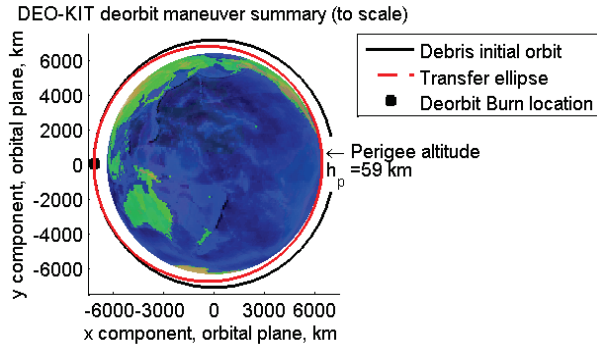


Fig. 7: DEO-Kit de-orbiting maneuver summary.

IV. DEBRIS CAPTURE AND MATING

The debris capture strategy is based upon the employment of two grasping systems which operate in sequence: the first one (Soft Docking System) is in charge of establishing the initial contact with the object, damping the impact loads and compensating for the residual Chaser-target relative attitude motion at the end of the rendezvous phase; the second one (Hard Docking System) is committed to realize a strong structural connection between the Chaser and the debris, in order to withstand the propulsive loads during the de-orbiting maneuver.

On one hand, the Soft Docking System (Figure 8^{7,8,9}) exploits electrostatic adhesion to generate the requested contact forces between the target surface and flexible electrodes mounted on a deformable material substrate which guarantees a better adaptability and adhesion between the interfaces. A secondary component of the system is made of low rigidity passive damping joints which reduce impact forces and dissipate the relative velocities and oscillations between the debris and the Chaser vehicle after contact. The joints are based on elastomeric elements whose deformation determines internal energy dissipation. The main advantage of the proposed Soft Docking System is that the adhesion mechanism does not require any particular structural feature to perform the grasping: in case of rocket bodies it could fit to the surface of the divergent part of the nozzle, and in case of abandoned spacecraft it could fit to any external surface of the vehicle.

On the other hand, the Hard Docking System design is more dependent on the target: in case of abandoned rocket bodies, the gas dynamic nozzle may represent a good point for the Chaser connection, due to its high resistance to thermal, fluid dynamic and mechanical

strain. The Chaser and the de-orbiting kit can be therefore equipped with a special “corkscrew system” (see Figure 9), theoretically able to secure the HPM or the Chaser to the selected Cosmos-3M second stage¹⁰.

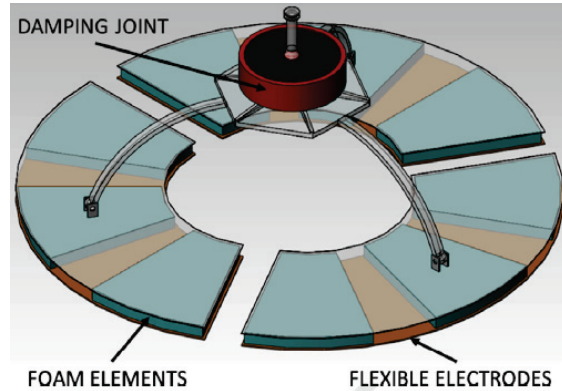


Fig. 8: Soft docking system schematic.

The corkscrew system is composed by a special titanium rod, which must be inserted inside the nozzle, centering the throat. Considering the Chaser (hence the second target), it must lean against the divergent nozzle border where the Soft Docking System connects to it. After completing the relative motion damping, the corkscrew mechanism can be activated, performing the mating with the internal walls of the convergent part of the nozzle. The mechanism consists of a threaded rod which moves four metal arms by cogwheels. This solution allows entering through the small throat diameter, thanks to the initial forward orientation of the arms.

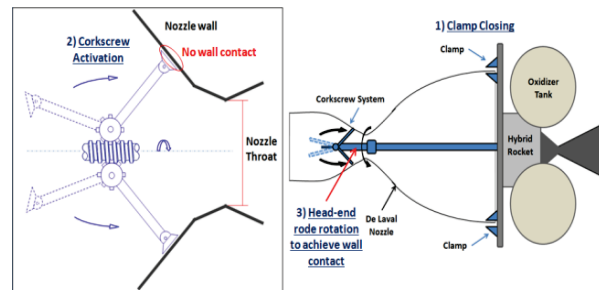


Fig. 9: Corkscrew system mechanism.

Then, activated by electric actuators, the four metal arms rotate back toward the internal convergent wall. At this point, the arms feet do not touch yet the nozzle surface (the erosion level of the wall is not known), thus a further rotation of only the head-end of the rode allows the arms feet to lean against the internal wall, involving a little compression of the nozzle, in order to keep it strictly connected to the Chaser. The same mechanism is used to attach the de-orbiting kit to the nozzle of the first target, but, in this case, a robotic arm

transfers the de-orbiting kit from the Chaser to the Cosmos-3M second stage. No stress or structural analysis has been yet performed about the corkscrew system, so it is still a conceptual idea. A possible critical point could be represented by the concentrated stresses in correspondence of the four arms during the HPM thrust phase. Different solutions for the corkscrew terminal component may be investigated.

In summary, starting from the contact time instant, the capture procedure occurs as following. At the beginning of the capture sequence, the adhesive material is activated and put in contact with the debris surface. The polymeric foam substrate adapts to the local features of the target, the attraction force is established and the two bodies are softly connected. Preliminary estimations show that attraction pressures up to 10 kPa normally and up to 4 kPa in shear are feasible. In this phase the damping joint plays a key role in reducing the impulsive loads in the systems, thus reducing the requisites of the adhesion system and increasing the chances of a successful docking. In the next phase, the two objects move together with a residual relative velocity. The damping joint dissipates the relative kinetic energy and the oscillations decay over time. After the relative motion is completely damped, the Chaser attitude control system de-tumbles the two body system. Once, the mated system attitude is stabilized, the hard docking between the debris and the Chaser or the de-orbiting kit, in the case of the first target, becomes possible.

V. HYBRID ROCKETS SIZING AND SYSTEM MASS BUDGET

V.I Hybrid Propulsion Engines

The target size, the disposal strategy and the propulsion technology are important aspects with a strong impact on mass budget, system volume, and cost of the propulsion unit. Considering a large object, the capability of throttling and re-ignition may represent a stringent requirement for the adequate control of the disposing maneuver, whereas compact design is important for easier docking to the target and for dynamic stability of the final assembly (Chaser and target). Compact volume may request a higher average propellant density but may collide with the ΔV requirements for a controlled atmospheric reentry, needed for large systems, orbiting at the highest altitudes. Thrust level should stem from a trade-off choice about the risk of debris fragmentation, especially for large objects, and long mission duration (correlated to propellant storability and collision risk during maneuver). Several innovative proposals are under development nowadays with varying time frames of realization; however, most of them need in-orbit demonstration of reliability and applicability on a real mission. Out of this group, it is worth mentioning the

use of tethers, as single spaceships as well as in fleet, to perform uncontrolled de-orbiting even of multiple targets^{11,12}. Other options, for the time being, appeal to systems already studied or realized in on-board de-orbiting devices, such as drag augmentation techniques (deployed sails or inflating balloons) or proven propulsion devices¹³. In this respect, a cost analysis for the de-orbiting of a 1.2 metric ton IRS-1C satellite was presented for different propulsion options, suggesting that chemical rockets can be a viable solution¹⁴. Among this pool of technologies, solid propellants represent a simple, reliable, and proven technology but feature low specific impulse, limited flexibility and not suitability for multi-burn missions, while liquid propellants fill the gaps left by the solid propellants, but larger volumes and higher degree of complexity are requested. Furthermore, storability of the propellant must be carefully considered, as well as the high toxicity of typical liquid substances used for space applications. Thus, hybrid rocket technology for de-orbiting applications is considered a valuable option due to the high specific impulse obtainable, intrinsic safety, possibility of green propellant use, low cost technology and, especially, re-ignition and thrust throttleability. The latter may be a key aspect to avoid the risk of fragmentation for the most fragile components of a large abandoned satellite, during the de-orbiting maneuver.

A hybrid rocket engine typically features the oxidizer in the liquid or gaseous state, while the fuel is in the solid state. Its safety is guaranteed by no-contact between fuel and oxidizer, except during the combustion phase. A hybrid rocket can also be built with a particular geometry, using a tangentially oxidizer injection, resulting very compact and highly efficient in combustion, thanks to the oxidizer flow which provides a vortex combustion. This particular kind of engine results very small in size. Such characteristics can be the right solution for space debris mitigation, by supplementing with this engine the new satellites that will reach space in the future. In our view, this technology is very promising even in the field of space debris remediation, making possible the active removal in LEO of large intact objects (several metric tons), both spacecraft and rocket bodies, by using one HPM for the reentry maneuver, equipped with several micro-thrusters, for the attitude control, spilling the HPM liquid oxidizer and burning it as a monopropellant (dual-mode use)^{7,15,16,17}. Overall, a hybrid propulsion module represents a solution that mediates benefits and drawbacks from both liquid and solid rocket technology. On one side, it is bestowed the throttleability and re-ignition capability typical of liquids, specific impulse levels which fall in between the performance of solid and liquid propulsion, and a higher mean propellant density due to the use of a solid fuel. Nevertheless, a technological gap exists due to late development and

lack of in-orbit demonstration.

In the simplest possible configuration, a hybrid rocket is made by a center-perforated solid fuel placed in the combustion chamber where an injector blows in a liquid or gaseous oxidizer. Low regression rate is the main drawback of this combustion process, but different means are considered for the enhancement of mass burning rate spanning from the use of advanced additives to different injection approaches (swirling oxidizer and vortex combustion)^{18,19}. Moreover, special advanced designs of the combustion chamber, such as vortex pancake, provides high combustion efficiency, low performance variation during combustion, and – in the case of solid metal additives – reduced emission of condensed combustion products thanks to the vortex effect²⁰.

For the preliminary sizing of the HPM, the attention was focused on HTPB (hydroxyl-terminated polybutadiene) as fuel and H₂O₂ as oxidizer. This combination of propellants provides ideal vacuum specific impulses (I_{s-vac}) over 300 s and significant volumetric specific impulses (I_v), due to the high density of the hydrogen peroxide⁷. In view of its good compromise between performance, costs and toxicity, hydrogen peroxide seems to be the best choice for this kind of application. In particular its catalytic decomposition provides oxygen-rich hot gases up to 1,000 K. Considering that ignition of HTPB solid fuel requires about 800 K, it is possible to develop a simple and reliable re-ignition system. Moreover, with a single tank of H₂O₂, it is possible to feed both the primary propulsion system and a set of Reaction Control System (RCS) catalytic micro-thrusters. Though hydrogen peroxide is notorious for its storability issues, due to its decomposition inside tanks, high level of peroxide purity and the use of appropriate materials have demonstrated that risks can be avoided and the rate of dissociation can be reduced appreciably²¹.

Hybrid technology allows managing the thrust level, by the supply of oxidizer mass flow rate, providing gradual accelerations during the initial transient phase. In fact, while for a rocket body, due to its structural design, the risk of fragmentation is low, a spacecraft, made by thin and light structures, having several appendages (i.e. antennas, solar panels, etc.), requires to be stressed by low accelerations, in order to avoid any possible breakup and the consequent generation of new debris.

A multi-removal mission requires a hybrid engine for each debris which we aim to remove. Considering two Cosmos-3M second stages, the best approach is to attach a hybrid propulsion module on the first target and use the hybrid rocket engine, the primary propulsion system of the Chaser spacecraft, for the second target, exploiting the remaining propellant. Two hybrid engines have to be preliminary designed. In order to evaluate a

preliminary hybrid rocket mass budget and size, the simplified regression rate equation from Marxman theory¹⁸ is considered:

$$r_f(t) = a_0 \left(\frac{4\dot{m}_o}{\pi D_p^2(t)} \right)^n \quad [3]$$

where \dot{m}_o is the oxidizer mass flow rate, D_p is the perforation diameter, while a_0 and n are coefficient evaluated experimentally. The fuel grain is cylindrical with a single central circular perforation. A zero-dimensional model is considered, assuming the same burning rate for the whole perforation surface, evaluated at the correspondence time step. With this simple approach, it is possible to estimate the fuel mass flow rate \dot{m}_f and, considering a constant oxidizer mass flow rate, the oxidizer-fuel mixture ratio OF at each time step:

$$\dot{m}_f(t) = \rho_f \pi L D_p(t) r_f(t) \quad [4]$$

$$OF(t) = \dot{m}_o / \dot{m}_f(t) \quad [5]$$

The hot gases are expanded through a conical De Laval nozzle and, by means of the CEA NASA software²² for the evaluation of thermo-chemical parameters which depend on combustion conditions, rocket performance are estimated. The selected propellant couple is HTPB + H₂O₂ (90%). A first preliminary check with mission requirements is performed evaluating the velocity increment under the hypothesis of equilibrium between centripetal and centrifugal forces, with no atmospheric and solar radiation drags. This iterative process carries on, by changing the fuel grain size, the oxidizer mass flow rate, the nozzle throat diameter and combustion time, as long as the required velocity increment is reached. Finally, the thrust profile evaluated is used for the trajectory simulation and maneuver feasibility analysis.

The first one is the HPM which is the main component of the de-orbiting kit, made even by a hard docking system and a RCS for the attitude control during the disposal. The required velocity increment estimated for the de-orbiting and controlled reentry of the target is about 200 m/s (this value is the highest ΔV between the two targets, chosen for the sizing) and, in order to take into account the losses due to the gas dynamic nozzle and the low efficiency of hybrid combustion, a ΔV increase of 25% is applied. Proper experiments about combustion configurations and engine firing tests will provide the effective performance parameters for different injection and geometrical chamber design solutions. Considering one burn of 52 s, it is possible to de-orbit the selected target by placing it on an elliptic trajectory with a FPA equal

to -1.7° at the 120 km atmospheric interface, corresponding to a nominal perigee at an altitude of 59 km. From a preliminary design, the HPM results with a mass of 160 kg, including the propellant mass, generating an average thrust of 6.2 kN with an average acceleration on the system (HPM + debris) of 0.42 g. The vacuum specific impulse results about 320 s. Reducing the oxidizer mass flow rate, making two burns of about 45 s, it is possible to obtain lower thrust levels, approximately 4 kN with 0.28 g of acceleration. The external diameter of the rocket is 21 cm, while the total length (including the submerged nozzle) is 136 cm. If the oxidizer tanks are placed at the sides of the rocket (Figure 10), the HPM maximum width is about 101 cm. For a better mass distribution and a more compact configuration, four spherical tanks (Figure 10), having an external diameter of 40 cm, with an internal elastomeric membrane for pressurization with gaseous N_2 , are considered. However, with the aim of cost lowering, two lateral cylindrical tanks would be preferable.

The ignition of the HPM system is performed by catalytic cells in which the hydrogen peroxide decomposes, generating oxygen-rich hot gases, then expanded in the combustion chamber. In order to limit the hydrogen peroxide natural decomposition, hence the hazard risk, high purity aluminum tanks are recommended²³. This HPM sizing takes into account even the mass of the RCS for attitude control during the de-orbiting. Because of the increase of oxidizer to fuel ratio (O/F) during the combustion, hence oxygen-rich exhaust gases, a nozzle made by phenolic material is preferable, due to its better resistance compared to graphite.

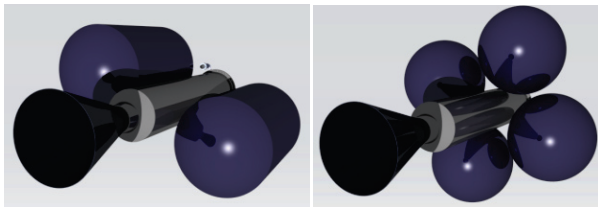


Fig. 10: HPM conceptual sketch with a 2 cylindrical tanks configuration (left) and a 4 spherical tanks configuration (right).

Concerning the preliminary design of the HRE, which is the Chaser primary propulsion system, the total velocity increment required takes into account 96 m/s of RV maneuvers, as well as the ΔV for the disposal, 200 m/s. A margin increase of 25% has been applied. The Chaser spacecraft is composed by the HRE, a Chaser bus and one de-orbiting kit. From preliminary system consideration and historical data relevant to similar missions, the Chaser bus has been estimated having a mass of 845 kg. The resulting mass of the de-orbiting

kit is about 200 kg, including the HPM, the hard docking system and the needed avionics.

Considering one burn of 63 s, it is possible to de-orbit the second Cosmos-3M stage by placing it on an elliptic trajectory with a FPA equal to -1.8° at the 120 km atmospheric interface, corresponding to a nominal perigee at an altitude of 52 km.

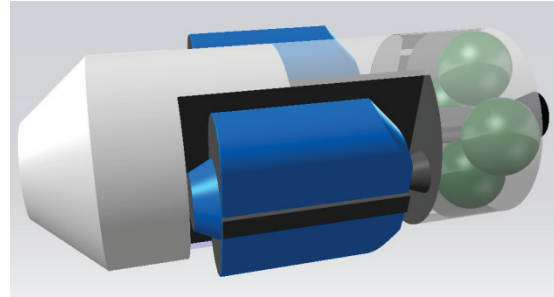


Fig. 11: Possible Chaser spacecraft conceptual sketch with two de-orbiting kit loaded (blue), HPMs with two cylindrical tanks. The HRE is inserted into the Chaser body structure.

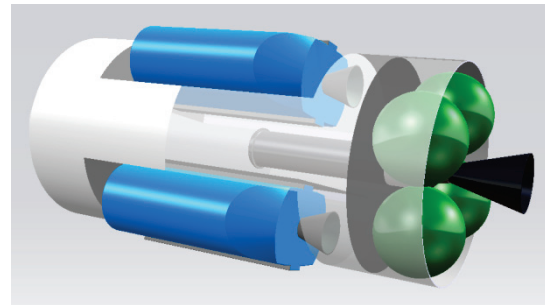


Fig. 12: Possible Chaser spacecraft conceptual sketch with two de-orbiting kit loaded (blue), HPMs with two cylindrical tanks. Rear view of the HRE green tanks and nozzle.

From the preliminary design, the HRE results with a mass of 305 kg, including the propellant mass, generating an average thrust of 8.4 kN with an average acceleration on the system of 0.35 g during the de-orbiting phase, while, during RV maneuvers, an average thrusts of 4.3 kN with average accelerations on the system of 0.37 g are estimated. The I_{s-vac} results about 320 s. The external diameter of HRE is 25 cm, while the total length (including the submerged nozzle) is 162 cm. Placing the oxidizer tanks at the sides of the rocket, the HRE maximum width is about 126 cm. For a better mass distribution and a more compact configuration, four spherical tanks, having an external diameter of 51 cm, are placed in the bottom part of the combustion chamber, near the nozzle. So the combustion chamber is inserted in the Chaser body. Both HRE and HPM use a conical nozzle made by phenolic material, with an area

ratio of 50 to keep small sizes. In Figures 11 and 12, one can see the conceptual sketch of a possible in scale configuration for the hybrid engines assembled on the Chaser: the HRE is represented with four green spherical tanks, while, in order to reduce the Chaser maximum width, two cylindrical tanks are considered for the HPM (de-orbiting kit with blue case). The conceptual sketch has an explicative purpose, showing the size and configuration differences between the hybrid engines designed. In Figures 11 and 12, just for representative purpose, two de-orbiting kit are shown.

V.II System Mass Budget

Given the mission profile and the ΔV budgets for RV and de-orbiting, a preliminary estimate of the Chaser mass can be performed. More specifically, if we indicate with ΔV_1 , ΔV_2 and ΔV_3 the velocity increments needed for the RV operations and the de-orbiting of the Chaser mated with the second target stage, the corresponding Mass Ratios (MR) can be computed as:

$$MR_i = e^{\frac{\Delta V_i}{I_{sp}g}} \quad i = 1,2,3 \quad [6]$$

being I_{sp} the specific impulse and g the gravity acceleration. As well known, the ratio of the propellant consumption to the initial mass for each maneuver can be expressed as:

$$\frac{m_{p_i}}{m_{ini}} = 1 - \frac{1}{MR_i} \quad i = 1,2,3 \quad [7]$$

with

$$\begin{aligned} m_{in1} &= m_{CB} + m_{HRE} + m_{DKit} + m_{p1} + m_{p2} + m_{p3} \\ m_{in2} &= m_{in1} - m_{DKit} - m_{p1} \\ m_{in3} &= m_{in2} + m_{Debris} - m_{p2} \\ m_{DKit} &= m_{HPM} + m_{AV} \end{aligned} \quad [8]$$

being m_{in1} the Chaser mass at the first RV starting, m_{in2} the Chaser mass at the second RV starting and m_{in3} the system mass at the Chaser disposal starting, i.e. when the Chaser is mated with the second debris target. Instead, m_{CB} is the Chaser bus mass, m_{HRE} is the Chaser main engine inert mass, and m_{DKit} is the mass of the de-orbiting kit carried by the Chaser and installed on the first target. This last one includes the HPM, as well as all the systems and avionics necessary for debris capture and controlled reentry. For preliminary mass budget, the HPM and HRE inert masses can be expressed as a fraction, k , of their total mass (i.e. including propellant), which yields:

$$m_{HRE} = \left(\frac{k}{1-k}\right) (m_{p1} + m_{p2} + m_{p3}) \quad [9]$$

$$m_{HPM} = \frac{1}{1-k} m_{p4} \cong \frac{1}{1-k} m_{Debris} \left(1 - \frac{1}{MR_4}\right) \quad [10]$$

where m_{p4} is the propellant consumed for the disposal of the first target, computed by neglecting the de-orbiting kit mass with respect to the target mass, and MR_4 is the mass ratio relevant to the first target disposal. After some mathematics, the Chaser mass can be computed as a function of the Chaser bus and debris mass as follows:

$$m_{in1} = \frac{m_{CB} + (ab+c)m_{Debris} + bm_{AV}}{d} \quad [11]$$

where

$$\begin{aligned} a &= \frac{1}{1-k} \left(1 - \frac{1}{MR_4}\right) \\ b &= 1 - \left(1 + \frac{k}{1-k}\right) \left(1 - \frac{1}{MR_2 MR_3}\right) \\ c &= \left(1 + \frac{k}{1-k}\right) \left(1 - \frac{1}{MR_3}\right) \\ d &= 1 - \left(1 + \frac{k}{1-k}\right) \left(1 - \frac{1}{MR_1 MR_2 MR_3}\right) \end{aligned} \quad [12]$$

Assuming for k typical values (i.e. 0.3), the Chaser initial mass is about 1370 kg, i.e. about 49% of the total removed mass (i.e. 2800 kg), and within the capability of a small launcher as VEGA. The de-orbiting kit and HRE masses are about 193 kg and 330 kg, respectively. These values are in good agreement with the estimates of the previous section, and suggest that the removal of up to 3 targets per year might be feasible with an active debris removal system fitting a VEGA-class launcher.

VI. CONCLUSIONS

The active removal of large debris, such as the second stage of Cosmos-3M, is a complex operation requiring the combination of several advanced technologies. In this paper, some critical aspects related to a demonstration mission for the removal of two Cosmos stages have been investigated at a preliminary level. The first removal is performed by installing a de-orbiting kit on the first target, consisting of an autonomous propulsion module with the needed avionics. Instead, the second removal is achieved by using the main engine of the removal platform while it is rigidly connected to the second target. A crucial aspect of such a mission is the selection of a suitable propulsion system. In this regard, the paper demonstrates that the hybrid rocket technology can be a viable option, since its high performance and flexibility allows performing both removal system rendezvous operations and debris disposal. In particular, this last one can be performed in a controlled fashion, thus minimizing the risks at ground. System analyses, performed with reference to a preliminary mission profile, show that the de-orbiting kit mass is about 200 kg, whereas the removal platform main engine wet mass is about 305 kg. The removal system total mass is about

1350 kg (i.e. 48% of the total removed mass), and within the capability of a small launcher as VEGA, showing that the removal of up to 5/3 targets per year might be feasible with a single mission using a heavy launcher/small launcher.

REFERENCES

1. DeLuca, L.T., et al. 2013. Active removal of large massive objects by hybrid propulsion module, Paper ID 469, in *5th European Conference for Aero-Space Sciences* (EUCASS 2013), ISBN 978-84-941531-0-5 (DVD).
2. Anonymous. 2012. Monthly mass of cataloged objects in Earth orbit by object type, *Orbital Debris Quarterly News*, 16(2), 10.
3. Liou, J.-C. 2011. An active debris removal parametric study for LEO environment remediation, *Advances in Space Research*, 47, 1865–1876.
4. IADC Steering Group & Working Group 4 (Mitigation). 2007. IADC space debris mitigation guidelines. Report IADC-02-01, rev. 1. Inter-Agency Space Debris Coordination Committee (IADC).
5. Liou, J.-C., Johnson, N.L. 2009. A sensitivity study of the effectiveness of active debris removal in LEO, *Acta Astronautica*, 64, 236–243.
6. Bastida Virgili, B., Krag, H. 2009. Strategies for active removal in LEO, *Proceedings of the 5th European Conference on Space Debris*, ESA SP-672, CDROM, European Space Agency, Noordwijk, The Netherlands.
7. DeLuca, L.T., Bernelli, F., Maggi, F., Tadini, P., Pardini, C., Anselmo, L., Grassi, M., Pavarin, D., Francesconi, A., Branz, F., Chiesa, S., Viola, N., Bonnal, C., Trushlyakov, V., Belokonov, I. 2012. Active space debris removal by a hybrid propulsion module, *Acta Astronautica*, doi: 10.1016/j.actaastro.2012.03.024.
8. Branz, F., et al. 2012. Innovative technologies for non-cooperative targets close inspection and grasping. In: *Proceeding of the 63rd International Astronautical Congress*. DVD, ISSN 1995-6258. International Astronautical Federation.
9. Branz, F., et al. 2013. Soft docking system for capture of irregularly shaped, uncontrolled space objects. In: *Proceedings of the 6th European Conference on Space Debris*.
10. Tadini, P., Maggi, F., DeLuca, L.T., Anselmo, L., Pardini, C., Grassi, M., Trushlyakov, V. 2012. Active debris removal of a Cosmos-3M second stage by hybrid rocket module. In: *VIII International Science and Technology Conference "Dynamics of Systems, Mechanisms and Machines"*, ISBN 978-5-8149-1350-0 (Book 2), pp. 218-237.
11. Bombardelli, C., et al. 2010. Electrodynamic tethers for space debris removal. In: *Space Debris Mitigation Workshop*.
12. Ohkawa, Y., et al. 2012. Electrodynamic tether (EDT) propulsion for LEO debris de-orbit. In: *Proceedings of the 2nd European Workshop on Active Debris Removal*, CNES HQ.
13. Trushlyakov, V. 2010. Development of means for space debris de-orbiting on the basis of separating parts of upper stages of the space launcher vehicle with liquid propulsion engine. In: *Beijing Orbital Debris Mitigation Workshop*.
14. Burkhardt, H., et al. 2002. Evaluation of propulsion systems for satellite end of life de-orbiting. AIAA Paper 4208.
15. DeLuca, L.T., et al. 2012. Active space debris removal by hybrid propulsion module, research project proposal to the Italian Ministry of Education, University and Research (MIUR).
16. DeLuca, L.T., et al. 2012. Active space debris removal by hybrid rocket propulsion. In: *Proceedings of the 2nd European Workshop on Active Debris Removal*, CNES HQ.
17. De Luca, L.T., et al. 2012. Active space debris removal by hybrid engine module. In: *Proceeding of the 63rd International Astronautical Congress*. DVD, ISSN 1995-6258. International Astronautical Federation. Paper IAC-12-A6.5.8.
18. Chiaverini, M.J., Kuo, K.K. 2007. *Fundamentals of hybrid rocket combustion and propulsion*, AIAA Progress in Astronautics and Aeronautics, Volume 218, pp. 37-116, 457-485.
19. Czysz, P., Bruno, C. 2006. *Future spacecraft propulsion systems: Enabling technologies for space exploration*, Springer Praxis.
20. Gibbon, D.M., Haag, G.S. 2001. Investigation of an alternative geometry hybrid rocket for small orbit transfer, Report SPBB-26287-01, Surrey Satellite Technology Limited.
21. Ventura, M., Wernimont, E., Heister, S., Yuan, S. 2007. Rocket grade hydrogen peroxide (RGHP) for use in propulsion and power devices. Historical discussion of hazards. AIAA Paper 5468.
22. Gordon, S., McBride, B.J. 1994. Computer Program of Complex Chemical Equilibrium Compositions and Applications (Part I), NASA Reference Publications, 1311.
23. Anonymous. 2010. Hydrogen peroxide (H₂O₂) safe storage and handling. Technical information papers and useful methods. TAPPI Standard TIP 0606-24, p. 8.